

Q1 The mixed serotonin receptor agonist psilocybin reduces threat-induced 2 modulation of amygdala connectivity

3 Rainer Kraehenmann^{a,b,*}, André Schmidt^{c,d}, Karl Friston^e, Katrin H. Preller^b,
4 Erich Seifritz^a, Franz X. Vollenweider^b

5 ^aDepartment of Psychiatry, Psychotherapy and Psychosomatics, Psychiatric Hospital, University of Zurich, Zürich 8032, Switzerland

6 ^bNeuropsychopharmacology and Brain Imaging, Department of Psychiatry, Psychotherapy and Psychosomatics, Psychiatric Hospital, University of Zurich, Zürich 8032, Switzerland

7 ^cDepartment of Psychiatry (UPK), University of Basel, Basel 4012, Switzerland

8 ^dDepartment of Psychosis Studies, Institute of Psychiatry, Psychology and Neuroscience, King's College London, London SE5 8AF, United Kingdom

9 ^eWellcome Centre for Imaging Neuroscience, University College London, London WC1N 3BG, United Kingdom

10 A R T I C L E I N F O

11 Article history:

12 Received 16 June 2015

13 Received in revised form 27 July 2015

14 Accepted 17 August 2015

15 Available online xxx

16 Keywords:

17 Serotonin

18 Psilocybin

19 Depression

20 fMRI

21 Dynamic causal modeling

A B S T R A C T

Stimulation of serotonergic neurotransmission by psilocybin has been shown to shift emotional biases away from 22 negative towards positive stimuli. We have recently shown that reduced amygdala activity during threat processing 23 might underlie psilocybin's effect on emotional processing. However, it is still not known whether psilocybin 24 modulates bottom-up or top-down connectivity within the visual-limbic-prefrontal network underlying 25 threat processing. We therefore analyzed our previous fMRI data using dynamic causal modeling and used Bayesian 26 model selection to infer how psilocybin modulated effective connectivity within the visual-limbic-prefrontal 27 network during threat processing. First, both placebo and psilocybin data were best explained by a model in 28 which threat affect modulated bidirectional connections between the primary visual cortex, amygdala, and lateral 29 prefrontal cortex. Second, psilocybin decreased the threat-induced modulation of top-down connectivity from 30 the amygdala to primary visual cortex, speaking to a neural mechanism that might underlie putative shifts to- 31 wards positive affect states after psilocybin administration. These findings may have important implications 32 for the treatment of mood and anxiety disorders. 33

© 2015 Published by Elsevier Inc. This is an open access article under the CC BY-NC-ND license (<http://creativecommons.org/licenses/by-nc-nd/4.0/>).

30

38

40 1. Introduction

41 Serotonin (5-hydroxytryptamine, 5-HT) is an important neuro- 42 transmitter within neural networks related to emotion processing. 43 We have recently shown that 5-HT_{2A} receptor activation by psilocybin 44 (4-phosphoryloxy-N,N-dimethyltryptamine) attenuates amygdala acti- 45 vation in response to threat-related visual stimuli in healthy volunteers 46 and that the reduction of amygdala blood oxygen level-dependent 47 (BOLD) signal is related to psilocybin's mood-enhancing effect 48 (Kraehenmann et al., 2014). Here, we addressed the hypothesis that 49 connectivity changes between the amygdala (AMG) and visual and 50 prefrontal cortical (PFC) areas contribute to the observed effects of 51 psilocybin on threat processing previously observed (Kraehenmann 52 et al., 2014). This hypothesis is based on evidence showing that the

processing of threat-related visual stimuli may be modulated via 53 feedback connections from the amygdala to the visual cortex (Furl 54 et al., 2013). Such top-down input from the amygdala to the visual 55 cortex may be an important mechanism at the interface between 56 emotion processing and visual perception – given that the amygdala 57 has been implicated in tuning visual processing to allocate resources 58 towards sensory processing of – and coordinating responses to – emo- 59 tionally salient stimuli (Morris et al., 1998). Furthermore, processing of 60 threat signals may be modulated via inhibitory feedback connections 61 from the PFC to the AMG (Hahn et al., 2011; Aznar and Klein, 2013). 62 Using DCM for fMRI, Sladky et al. (2015) recently analyzed the effects 63 of the selective serotonin reuptake inhibitor (SSRI) (S)-citalopram on 64 amygdala–PFC effective connectivity in healthy volunteers. They found 65 that the PFC exhibited a down-regulatory effect on amygdala activation, 66 and that this effect was significantly increased by the antidepressant 67 (S)-citalopram. Importantly, the inhibitory feedback from the PFC to the 68 AMG has been found to be correlated with 5-HT_{2A} receptor stimulation 69 (Fisher et al., 2009). Therefore, it is conceivable that the psilocybin- 70 induced attenuation of amygdala activation (Kraehenmann et al., 2014) 71

* Corresponding author at: Neuropsychopharmacology and Brain Imaging, Department of Psychiatry, Psychotherapy and Psychosomatics, Psychiatric Hospital, University of Zurich, Lenggstrasse 31, Zürich CH-8032, Switzerland. Tel.: +41 44 384 2827.

E-mail address: r.kraehenmann@bli.uzh.ch (R. Kraehenmann).

might be caused by increased inhibitory connectivity from the PFC to the AMG. Finally, given the abundance of feed-forward projections from visual input regions (e.g. primary visual cortex, V1) to the AMG (Pessoa and Adolphs, 2010) and from the AMG to the PFC (Volman et al., 2013), bottom-up connectivity changes may also contribute to psilocybin's effects on threat processing.

To test these hypotheses, we analyzed the functional magnetic resonance imaging (fMRI) data of our previous study (Kraehenmann et al., 2014) using dynamic causal modeling (DCM) (Friston et al., 2003) and Bayesian model selection (BMS) (Stephan et al., 2009). DCM is a general framework for inferring hidden mechanisms at the neuronal level from measurements of brain activity such as fMRI. Recent studies have demonstrated its sensitivity to detect pharmacological manipulations in fMRI data (Grefkes et al., 2010; Schmidt et al., 2013b); in particular, after serotonergic stimulation (Volman et al., 2013). BMS is an essential aspect of DCM studies, as it can be used to test competing hypotheses (different DCMs) about the neural mechanisms generating data. We applied DCM and BMS to address the following questions: First, which is the most likely mechanism underlying threat processing, (1) threat-induced modulation of bottom-up connectivity, (2) threat-induced modulation of top-down connections, or (3) modulation of both bottom-up and top-down connections by threat stimuli. Secondly, which of these mechanisms – changes in bottom-up or top-down connectivity – contributed to the psilocybin-induced reduction of AMG (Kraehenmann et al., 2014) and V1 activation (Schmidt et al., 2013a) in response to threat-related visual stimuli.

2. Methods

2.1. Subjects

In total, 25 healthy, right-handed subjects (16 males, mean age 24.2 ± 3.42 years) with normal or corrected-to-normal vision were recruited through advertisements placed in local universities. Subjects were screened for DSM-IV mental and personality disorders using the Mini-International Neuropsychiatric Interview (Sheehan et al., 1998) and the Structured Clinical Interview II (First et al., 1997). Exclusion criteria were as follows: pregnancy, left-handedness, poor knowledge of the German language, personal or first-degree relatives with history of psychiatric disorder, history of alcohol or illicit drug dependence, current alcohol abuse or illicit drug use, current use of a medication that affects cerebral metabolism or blood flow, cardiovascular disease, history of head injury or neurological disorder, magnetic resonance imaging exclusion criteria (including claustrophobia), and previous significant adverse reactions to a hallucinogenic drug. Subjects were healthy according to medical history, physical examination, routine blood analysis, electrocardiography, and urine tests for drug abuse and pregnancy. The study was approved by the Cantonal Ethics Committee of Zurich (KEK). Written informed consent was obtained from all subjects and the study was performed in accordance with the Declaration of Helsinki.

2.2. Experimental design

As previously reported (Kraehenmann et al., 2014), the study design was randomized, double-blind, placebo-controlled, cross-over. Subjects received either placebo or 0.16 mg/kg oral psilocybin in two separate imaging sessions at least 14 days apart. The use of psilocybin was authorized by the Federal Office of Public Health, Federal Department of Home Affairs, Bern, Switzerland. Psilocybin and lactose placebo were administered in gelatin capsules of identical number and appearance. A 0.16-mg/kg dose of psilocybin was selected because it reliably induces changes in mood and consciousness, but minimally disrupts behavioral task performance and reality testing (Studerus et al., 2011). Mood state was assessed using the Positive and Negative Affect Schedule (PANAS) (Watson et al., 1988) and the state portion of the State–Trait

Anxiety Inventory (STAI) (Spielberger and Gorsuch, 1983) before and 210 min after each drug treatment. The scanning experiment was conducted between 70 and 90 min after drug administration to coincide with the plateau in the subjective effects of psilocybin (Hasler et al., 2004). Subjects were released about 360 min after drug administration, after all acute drug effects had completely subsided.

2.3. fMRI paradigm: amygdala reactivity task

Inside the scanner, subjects performed an amygdala reactivity task comprising alternating blocks of emotional (threat and neutral) picture discrimination tasks. The picture discrimination task was interspersed with shape discrimination tasks, which served as baseline tasks and allowed amygdala responses to return to baseline.

Stimulus material for the amygdala reactivity task was obtained from the International Affective Picture System (IAPS), a standardized and broadly validated collection of emotionally evocative pictures (Lang et al., 2005). Stimulus sets of 48 different pictures were arranged in picture-triplets on a gray background. The stimulus triplets comprised the target picture in the upper center position, and two pictures as potential matching targets on the left and right sides at the bottom of the slide. Twenty-four pictures were categorized as threat and 24 as neutral. The threat pictures were aversive, threat-related pictures such as attacking animals, aimed weapons, car accidents, and mutilations, and the neutral pictures depicted activities of daily living, portraits of humans and animals, and everyday objects.

During the emotional picture discrimination task, subjects were required to select one of the two IAPS pictures at the bottom of the stimulus triplet that matched the target picture at the top of the triplet. Selection was indicated by pressing one of two buttons on a magnetic resonance (MR)-compatible response device with the dominant hand. A shape discrimination task was performed as a sensorimotor control and baseline task. This required matching of geometric shapes (circles, ovals, and rectangles) analogous to the picture discrimination task and was implemented to control for activation due to non-emotional cognitive and visual processing. Both tasks were shown as alternating 24-s blocks without intermittent pauses. Each block was preceded by a 2-s instruction (“Match Pictures” or “Match Forms”) and consisted of six target images that were presented sequentially for a period of 4 s in a randomized order. The experimental design comprised four repetitions of the sequence threat → shapes → neutral → shapes, cumulating to a total duration of 420 s for the complete run. Individual trial durations were not determined by the subjects' responses, and no feedback was provided regarding correct or incorrect responses.

2.4. fMRI image acquisition and data analysis

Scanning was performed on a 3 T scanner (Philips Achieva, Best, The Netherlands) using an echo planar sequence with 2.5 s repetition time, 30 ms echo time, a matrix size of 80×80 and 40 slices without interslice gap, providing a resolution of $3 \times 3 \times 3$ mm³ and a field of view of 240×240 mm³.

Data analysis was performed with SPM12b (<http://www.fil.ion.ucl.ac.uk>). All volumes were realigned to the mean volume, co-registered to the structural image, normalized to the Montreal Neurological Institute space using unified segmentation (Ashburner and Friston, 2005) including re-sampling to $3 \times 3 \times 3$ mm voxels, and spatially smoothed with an 8-mm full-width at half-maximum Gaussian kernel. First-level analysis was conducted using a general linear model applied to the time series, convolved with a canonical hemodynamic response function (Friston et al., 1994). Serial correlations and low-frequency signal drift were removed using an autoregressive model and a 128-s high-pass filter, respectively. Single-subject GLM analysis for the two sessions (placebo and psilocybin) comprised regressors for threat, neutral pictures, and shapes. These conditions were modeled as box-car

193 regressors representing the onset of each block type. Subject-specific
194 condition effects for threat minus shapes were computed using
195 t-contracts, producing a contrast image for each subject that was used
196 as a summary statistic for second-level (between subject) analyses.

197 2.5. Dynamic causal modeling (DCM)

198 The current DCM analyses (version 12 with SPM12b) are based on
199 the GLM analyses of the fMRI data described above (Kraehenmann
200 et al., 2014). In DCM for fMRI, the dynamics of the neural states under-
201 lying regional BOLD responses are modeled by a bilinear differential
202 equation that describes how the neural states change as a function of
203 endogenous interregional connections, modulatory effects on these
204 connections, and driving inputs (Friston et al., 2003). The endogenous
205 connections represent constant coupling strengths, whereas the
206 modulatory effects represent context-specific and additive changes in
207 coupling (task-induced alterations in connectivity). The modeled
208 neuronal dynamic is then mapped to the measured BOLD signal using
209 a hemodynamic forward model (Stephan et al., 2007). We explicitly
210 examined how the coupling strengths between V1, AMG, and PFC are
211 changed by threat during the AMG reactivity task (modulatory effect).

212 2.5.1. Regions of interest and time series extraction

213 We selected three regions of interest (ROIs) within a right-
214 hemispheric network implicated in visual threat processing, based on:
215 (1) previously published conventional SPM analyses of these data
216 (Fig. 1) (Kraehenmann et al., 2014), (2) previous anatomical and struc-
217 tural connectivity studies (Freese and Amaral, 2005), and (3) previous
218 DCM studies of threat processing using visual stimuli (Volman et al.,
219 2013). In DCM for fMRI, a neural network is analyzed in terms of direct-
220 ed connectivity changes among selected regions of interest. Regions of
221 interest are selected based on both a priori knowledge and hypotheses,
222 and on significant task-induced activations. We chose a right-
223 hemispheric (subgraph) analysis based on our previous GLM analysis
224 of psilocybin effects on threat processing (see Table 1, Fig. 3A and B)
225 (Kraehenmann et al., 2014). The rationale for this choice was to ask
226 whether the observed psilocybin-induced decrease of right amygdala
227 activation in response to threat was mediated by top-down connectivity
228 changes from the right prefrontal cortex or by bottom-up connectivity
229 changes from the right visual cortex. In addition, we limited our DCM
230 analyses to a right-hemispheric network or subgraph in view of statisti-
231 cal efficiency: it is common practice to test only a small number of
232 regions of interest with DCM. Future DCM studies of psilocybin effects
233 on threat processing could include the contralateral homologues of
234 the regions investigated here, although our previous GLM analysis did
235 not motivate a DCM analysis of the left-hemispheric network.

236 The ROIs included: rV1 ($x = 12, y = -82, z = -7$), rAMG ($x = 24,$
237 $y = -1, z = -13$), and the right inferior frontal gyrus within the lateral
238 PFC (rLPFC) ($x = 54, y = 32, z = 20$). The coordinates for the rV1, rAMG
239 and rLPFC were based on the contrast of threat pictures minus shapes.

240 Regional time series from each subject and session were extracted from
241 (10 mm) spherical volumes of interest centered on the suprathreshold
242 voxel nearest the group maxima. Time series were summarized with
243 the first eigenvariate of voxels above a subject-specific F threshold of
244 $p < 0.01$ (uncorrected) within the anatomical areas, as defined by the
245 Pick Atlas toolbox. During time series extraction it may happen that a
246 subject does not show activation at the group maximum and that the
247 nearest suprathreshold voxel lies outside the anatomical regions. By
248 additionally using an anatomical mask, we ensured that time series
249 were extracted from within a certain distance of the group maxima
250 (10 mm), but were not extracted from a region outside the anatomical
251 structure (Dima et al., 2011). We could not extract an rLPFC time series
252 in two subjects due to lack of individual activations fulfilling both the
253 above functional and anatomical criteria. Although it is not necessary to
254 preclude subjects who did not show significant activations from the
255 DCM analysis, the purpose of DCM is to explain observed activations in
256 terms of functional coupling. We therefore restricted our analyses to sub-
257 jects who showed significant responses under the assumption that their
258 data would provide more efficient estimators of connectivity.

259 2.5.2. DCM model space

260 First, we specified a three-area base model with bidirectional endog-
261 enous connections between V1 and AMG and between AMG and LPFC
262 (Fig. 2A). V1 was selected as the visual input region in our models. All
263 visual stimuli were used as inputs. These restrictions allowed us to
264 define a small model space. The basic model was then systematically
265 varied to provide alternative models of the modulatory effect (induced
266 by threat stimuli). The three model variants corresponded to the
267 three alternative hypotheses about modulatory effects (bottom-up,
268 top-down, or a combination of bottom-up and top-down) and allowed
269 us to distinguish between the three hypothesized mechanisms under
270 the two treatments (psilocybin, placebo) (Fig. 2B–D).

271 2.5.3. Model inference

272 Using random-effects BMS in DCM12, we computed expected prob-
273 abilities and exceedance probabilities at the group-level to determine
274 the most plausible of the three model variants for each drug (psilocybin,
275 placebo) separately (Penny et al., 2004). The expected probability of
276 each model is the probability that a specific model generated the data
277 of a randomly chosen subject, and the exceedance probability of each
278 model is the probability that this model is more likely than any other
279 of the models tested (Stephan et al., 2009). Bayesian model comparison
280 rests solely on the relative evidence for different models (as scored by
281 the variational free energy). This evidence comprises the accuracy
282 (i.e., percent variance explained) minus the complexity (i.e., degrees
283 of freedom used to explain the data). The evidence therefore reflects
284 the quality of a model in providing an accurate but parsimonious ac-
285 count of the data (and is preferred over conventional accuracy measures
286 that may reflect overfitting). Finally, we used random-effects Bayesian
287 model averaging (BMA) to compute (subject specific) connectivity

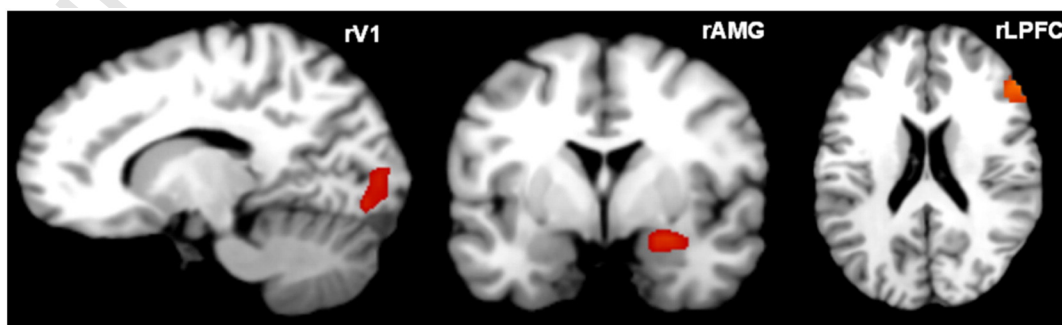


Fig. 1. Regional effects from the contrast of threat pictures minus shapes within right lateral prefrontal cortex (rLPFC; $z = 20$) and right amygdala (rAMG; $y = -1$) and from the contrast of all pictures (threat of non-threat) minus shapes within the right primary visual cortex (rV1; $x = 12$) across both drug conditions (placebo, psilocybin). SPM(t) overlaid on canonical brain slices (thresholded at $p < 0.001$ uncorrected for visualization).

Table 1
Dynamic causal modeling parameter estimates.

Connection	Endogenous		Modulation		Direct input	
	Pla	Psi	Pla	Psi	Pla	Psi
V1	+0.023 ± 0.05	−0.002 ± 0.01	−	−	+0.011 ± 0.12	−0.003 ± 0.01
V1 → AMG	+0.036 ± 0.08	+0.018 ± 0.05	+0.027 ± 0.37	+0.024 ± 0.09	−	−
AMG → V1	−0.028 ± 0.09	+0.031 ± 0.11	+0.526 ± 1.05	+0.030 ± 0.14*	−	−
AMG	−0.007 ± 0.02	−0.002 ± 0.01	−	−	−	−
AMG → LPFC	+0.005 ± 0.08	−0.005 ± 0.06	+0.103 ± 0.22	+0.023 ± 0.11	−	−
LPFC → AMG	−0.002 ± 0.05	+0.008 ± 0.00	−0.394 ± 1.12	−0.157 ± 0.76	−	−
LPFC	−0.014 ± 0.04	−0.001 ± 0.00	−	−	−	−

estimates (weighted by their posterior model probability) across all three models separately for psilocybin and placebo. This conservative analysis allowed the drug effect to be expressed in all connections and their threat related modulations, whereby we were able to establish significant effects in relation to intersubject variability using classical statistics at the between subject level.

2.5.4. Parameter inference

To evaluate the effect of psilocybin on endogenous connections and their modulation by threat stimuli, BMA values were entered into two separate 2-way repeated measures ANOVA with factors drug (psilocybin, placebo) and connection type (endogenous parameters: V1, V1 → AMG, AMG → V1, AMG, AMG → LPFC, LPFC → AMG, LPFC; modulatory parameters: V1 → AMG, AMG → V1, AMG → LPFC, LPFC → AMG). Where the ANOVA null hypothesis of equal means was rejected, we used the post-hoc test (Duncan's multiple range tests). A paired t test was further applied to compare direct inputs into V1 across both treatments. A p value of less than 0.05 was assumed as statistically significant.

2.5.5. Correlation with behavioral and mood measures

To investigate correlations between psilocybin-induced changes of effective connectivity and behavior or mood, the psilocybin-induced connectivity changes were correlated using Pearson correlations with

psilocybin-induced changes in behavioral measures (reaction time, accuracy) and mood scores (PANAS positive affect, PANAS negative affect, STAI state anxiety).

3. Results

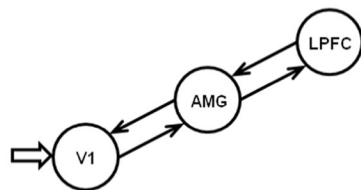
3.1. Model inference with Bayesian model selection

Under both psilocybin and placebo, the full model outperformed all other models with an exceedance probability of 97% (placebo) and 62% (psilocybin), respectively (Fig. 3). This optimal model comprised bidirectional endogenous connections between V1 and AMG, and between AMG and LPFC, with threat modulating both forward and backward connections.

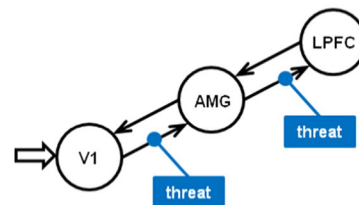
3.2. Parameter inference

To compare connectivity across drug treatments, the subject-specific parameter estimates were averaged over the three models for each treatment using BMA. The endogenous parameters, their threat induced modulations, and direct inputs from the BMA are shown in Table 1. Coupling or connectivity in dynamic models is measured in terms of Hz, where a strong baseline or endogenous connection would typically be between 0.1 and 0.5 Hz. This means that one can regard the effective connectivity as a rate-constant. In other words, a strong connection

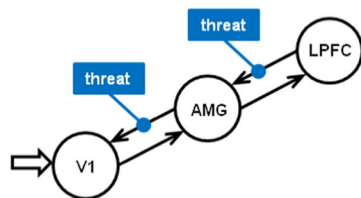
A: base model



B: bottom-up model



C: top-down model



D: full model

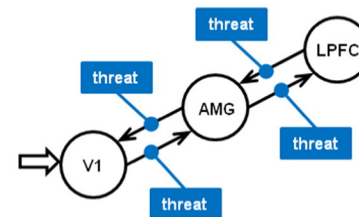


Fig. 2. Model specification. A, Basic structure of the three-area model: visual stimulus presentation drives V1 activity, which is bidirectionally connected to AMG, which in turn is bidirectionally connected to the LPFC. B, Bottom-up model: the modulatory effect of threat is only mediated via bottom-up connections from V1 to AMG to LPFC. C, Top-down model: the modulatory effect of threat is only mediated via top-down connections from LPFC to AMG to V1. D, Full model: the modulatory effect of threat is mediated via both bottom-up and top-down connections between V1 and AMG, and between AMG and LPFC.

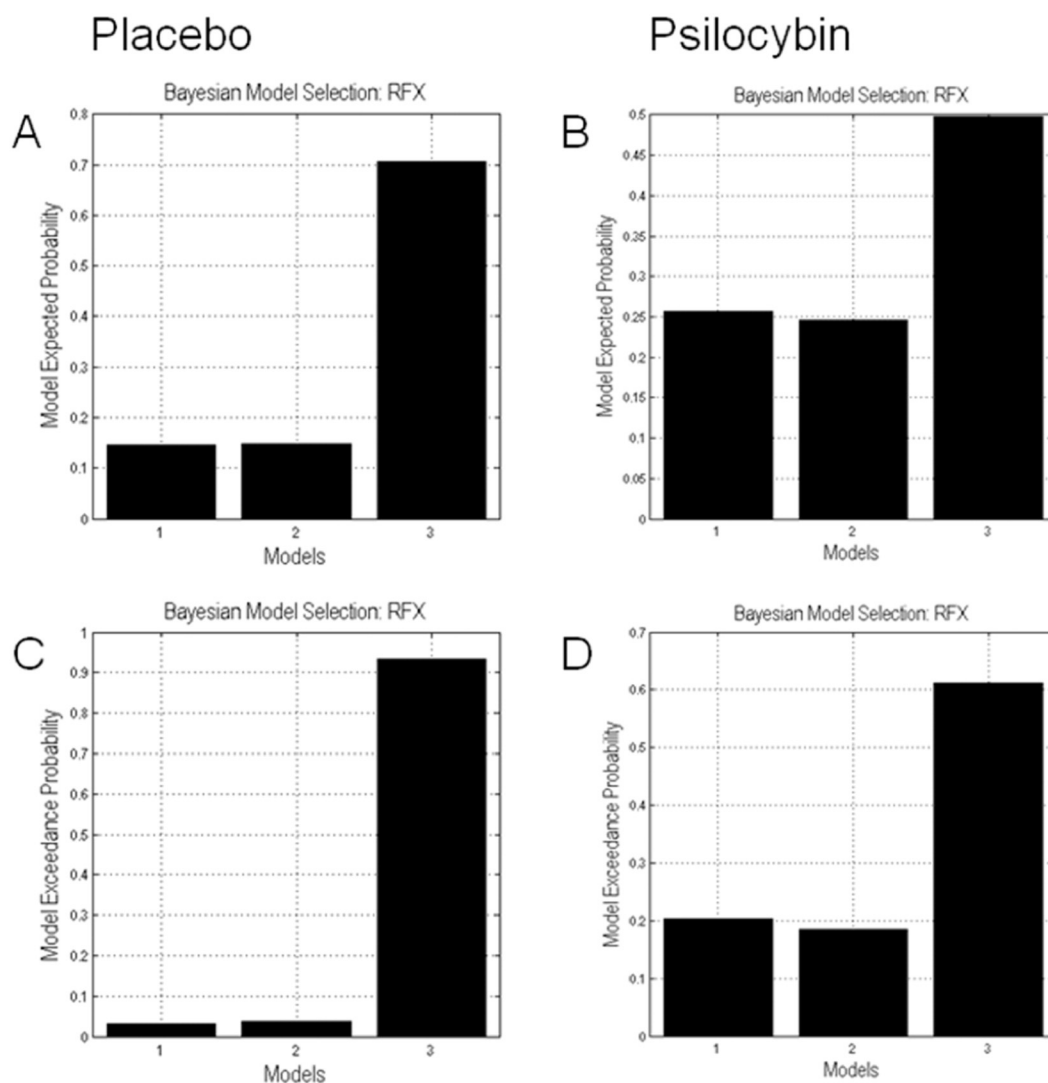


Fig. 3. Results of Bayesian model selection. Bar charts show the expected model probabilities (A, B) and exceedance probabilities (C, D) of the bottom-up model (1), the top-down model (2), and the full model (3) for the placebo (left) and psilocybin (right) treatment. Notably, the full model with threat-induced modulation of bidirectional connections is the winning model for both the placebo and psilocybin treatment.

330 causes a large rate of increase in the target region, with respect to
 331 activity in the source region. The inverse of the connection strength
 332 can therefore be interpreted in terms of a time constant (i.e., how long
 333 it would take for a source to increase activity in a target).

334 There was no main effect of drug ($F_{1,22} = 3.10$, $p = 0.09$, $\eta_p^2 = 0.12$),
 335 but a significant main effect of connection type ($F_{3,66} = 3.94$, $p = 0.01$,
 336 $\eta_p^2 = 0.15$), and a significant drug by connection type interaction
 337 ($F_{3,66} = 2.84$, $p = 0.04$, $\eta_p^2 = 0.11$) on modulatory coupling parameters.
 338 Post-hoc tests on the drug by connection type interaction showed that
 339 the threat-induced modulation of AMY \rightarrow V1 connectivity was signifi-
 340 cantly reduced after psilocybin compared to placebo administration
 341 ($p = 0.01$; Duncan's multiple range test corrected) (Table 1). There
 342 was no significant effect of psilocybin on endogenous or input param-
 343 eters (all $p > 0.05$).

344 Parameter estimates were obtained from Bayesian Model Averaging
 345 for placebo (Pla) and psilocybin (Psi), mean \pm standard deviation.
 346 Statistically significant differences between placebo and psilocybin
 347 treatments ($p < 0.05$ Duncan corrected for multiple comparison) are
 348 printed in bold and marked by an asterisk; V1 = primary visual cortex;
 349 AMG = amygdala; LPFC = lateral prefrontal cortex.

3.3. Correlation with behavioral and mood measures

350

We assessed correlations between (psilocybin–placebo) modulatory
 351 coupling changes for the AMG \rightarrow V1 connection from BMA and (psilocy-
 352 bin–placebo) changes of behavioral measures (reaction time, accuracy)
 353 and of mood scores (PANAS positive affect, PANAS negative affect, STAI
 354 state anxiety). We found no significant correlations (all $p > 0.05$).
 355

4. Discussion

356

In this study, we analyzed the fMRI data of our previous psilocybin
 357 study (Kraehenmann et al., 2014) using DCM, an established framework
 358 enabling tests of directed (effective) connectivity. We were interested
 359 whether psilocybin modulated effective connectivity within a network
 360 implicated in threat processing during an amygdala reactivity task. In
 361 particular, our aim was to differentiate between psilocybin-effects on
 362 bottom-up, top-down, and bidirectional connectivity during threat-
 363 processing within a visual–limbic–prefrontal network. There were two
 364 main findings from our study: Firstly, both placebo and psilocybin
 365 data were best explained by a model in which threat affect modulated
 366

bidirectional connections between V1, AMG, and LPFC. Secondly, psilocybin – compared to placebo – substantially reduced the modulatory effect of threat on the top-down connection from the AMG to V1. This implies that psilocybin attenuates amygdala-dependent top-down tuning of visual regions during threat processing.

Our BMS finding that the full model, which is characterized by bidirectional modulatory effects of threat on visual–limbic–prefrontal connectivity, outperformed both the bottom-up and the top-down model, is in line with previous DCM studies (Herrington et al., 2011; Goulden et al., 2012). In these studies, BMS consistently favored models, which implement modulatory effects on both bottom-up and top-down connections during negative emotion processing. The winning model in our study contained reciprocal connections between V1 and AMG (V1 ↔ AMG) and between AMG and LPFC (AMG ↔ LPFC). Both V1 ↔ AMG and AMG ↔ LPFC reciprocal connections are critically involved in negative-emotion processing (Herrington et al., 2011; Goulden et al., 2012). In fact, it has been shown that visual threat perception may be enhanced through a re-entry mechanism of feed-forward connections from V1 to AMG and feedback connections from the AMG to V1 (Herrington et al., 2011). Furthermore, visual threat perception may be increased through feed-forward connections from the AMG to LPFC (Lu et al., 2012) and attenuated through inhibitory feedback connections from the LPFC to AMG (Volman et al., 2013). Although BMS did not directly compare model fits from different datasets (e.g. placebo, psilocybin), our model selection results indicate a consistent mode of visual threat processing during placebo and psilocybin treatments; namely, via modulation of both bottom-up and top-down connectivity across the visual–limbic–prefrontal hierarchy.

Our main finding was that psilocybin (compared to placebo) reduced the modulatory effect of visual threat on the top-down connection from the AMG to V1. In both humans and animals, visual threat poses a strong salience signal, which needs to be processed efficiently and therefore binds attentional resources (Pessoa and Adolphs, 2010). The “tuning” of visual regions via feedback projections from the AMG during threat processing is an important mechanism underlying visual threat processing and may enhance perception of visual threat signals (Morris et al., 1998). In addition, the AMG has been closely linked to salience processing and may, via top-down predictive signals, guide bottom-up information processing (Vuilleumier, 2015). Therefore, the amygdala may actually determine the affective meaning of visual percepts by its effects on sensory pathways – an effect which mainly occurs subconsciously and which may be greatly amplified in psychopathological conditions, such as anxiety disorders or depression. In this context, increased AMG reactivity may lead to an increased attentional focus on negatively valenced environmental or social stimuli and thus effectively blocks out the processing of positive information (Disner et al., 2011). This is especially relevant for hallucinogenic drugs such as psilocybin, because there has been a close and psychotherapeutically interesting relationship between visual perception and affective processes during hallucinogen-induced states (Leuner, 1981). The psilocybin-induced attenuation of top-down threat signaling from the amygdala to visual cortex may therefore lead to decreased threat sensitivity in the visual cortex. This mechanism may crucially underlie the previously observed decrease of behavioral and electrophysiological responses in the visual cortex to threat stimuli during psilocybin administration (Vollenweider and Kometer, 2010; Schmidt et al., 2013a) and may explain the psilocybin-induced shifts away from negative towards positive valence during emotion processing (Kometer et al., 2012). In line with the notion that attenuation of the top-down connection from the AMG to visual cortex may reduce threat processing, a recent study showed that habituation to visual threat stimuli may parallel attenuation of top-down connectivity from the AMG to visual cortex (Herrington et al., 2011). In addition, it has been found that hyper-connectivity between the AMG and visual cortex may underlie increased threat processing and anxiety (Frick et al., 2013).

Given the relevance of LPFC in regulating AMG activity during threat processing, and given previous studies showing that serotonergic stimulation may increase inhibitory top-down connectivity from LPFC to AMG (Pessoa and Adolphs, 2010; Volman et al., 2013), we hypothesized that psilocybin-induced reduction in AMY activity might be due to an increased LPFC → AMG top-down connectivity during threat processing. However, psilocybin did not appear to increase top-down connectivity from LPFC to AMG in the current analysis. Two reasons might account for this. First, the source of the psilocybin-induced reduction of AMG activity, as observed in our previous GLM analysis (Kraehenmann et al., 2014), might not reflect an increased top-down effect from LPFC, but rather a suppression of recurrent interactions with visual areas mediated by a reduced top-down connectivity with the visual cortex. The synaptic basis of this reduced top-down modulation might reflect a direct effect of psilocybin in the amygdala: amygdala neurons abundantly express 5-HT_{2A} receptors, and DOI and other 5-HT_{2A} agonists produce direct effects in the amygdala (Rainnie, 1999). In addition, a directly decreased AMG reactivity would result in a reduced load on the LPFC to regulate AMG activation. This view is supported by a recent DCM study showing that increased AMG-related load on the PFC yields subsequent responses in the PFC to regulate the AMG (Volman et al., 2013). Second, the AMG might be regulated by prefrontal cortical regions other than the LPFC, such as the medial PFC (MPFC), the anterior cingulate cortex (ACC), or the orbitofrontal cortex (OFC), which have also been related to the ‘aversive amplification’ circuit (Robinson et al., 2013). For example, Sladky et al. (2015) recently analyzed the effects of the selective serotonin reuptake inhibitor (SSRI) (S)-citalopram on amygdala–OFC effective connectivity in healthy volunteers. They found that the OFC exhibited a down-regulatory effect on amygdala activation, and that this effect was significantly increased by the antidepressant (S)-citalopram. Although Sladky et al. used a similar threat-inducing amygdala reactivity task (Hariri et al., 2002) and likewise tested the effects in healthy volunteers, their study procedures differ substantially from our study, both in terms of task design (e.g. face stimuli instead of pictures, scrambled control stimuli, longer baseline conditions) and in terms of drug administration (e.g. chronic and repeated instead of acute and single treatment). Therefore, it is not easy to disambiguate task- from drug-specific effects in terms of PFC involvement and our DCM might have missed top-down effects from PFC on the AMG. However, given the cognitive task requirements in our task – where subjects were not explicitly required to evaluate or regulate their emotional responses to the threat stimuli – and given that the GLM analyses (Kraehenmann et al., 2014) did not show significant BOLD responses in the MPFC, ACC, or OFC, one might argue that top-down effects from other prefrontal regions are unlikely. Overall, both the hallucinogen psilocybin and the non-hallucinogen (S)-citalopram may normalize amygdala hyper-reactivity to threat-related stimuli; leading to their antidepressant and anxiolytic efficacy, but psilocybin appears to regulate emotion processing and mood by acting on network interactions which are different from classical antidepressants such as (S)-citalopram, such as the affective regulation of visual information processing shown here.

4.1. Limitations and future directions

There are some limitations to be considered in the present study. We used a fairly simplistic neuronal network underlying threat related effective connectivity. There are also other brain regions involved in threat processing, such as the ACC, the OFC, or the fusiform gyrus (Robinson et al., 2013), but that we did not include in our present model for reasons of parsimony and based on our a priori hypotheses. Furthermore, to maximize statistical efficiency, we only considered right-hemispheric networks in our DCM analyses. Therefore, top-down connectivity from the left LPFC to the right AMG might have been missed. Given the importance of the left LPFC in regulating the right AMG during emotion processing and in serotonergic modulation

497 (Outhred et al., 2013), we cannot exclude this possibility. Therefore, further
 498 effective connectivity studies using tasks that differentially recruit
 499 left and right prefrontal cortical regions during threat processing, are
 500 needed.

501 4.2. Conclusion

502 This effective connectivity study shows that a decrease of top-down
 503 connectivity from the AMG to the visual cortex underlies the psilocybin
 504 effect on visual threat processing. This result suggests that decreased
 505 threat sensitivity in the visual cortex during emotion processing may
 506 explain the potential of psilocybin to acutely shift emotional biases
 507 away from negative towards positive valence: the capacity of the visual
 508 cortex to process multiple stimuli is limited and hence top-down sup-
 509 pression of negative stimuli enhances the processing of positive stimuli
 510 (Kastner et al., 1998). This may have important therapeutic implications
 511 for mood and anxiety disorders, where over-loading with negative
 512 stimuli and persistence of negative cognitive biases is a central feature
 513 (Disner et al., 2011). In post-traumatic stress disorder, for example,
 514 psilocybin might help inhibit fear-responses during exposure-based
 515 psychotherapy, which might facilitate therapeutic progress.

516 Disclosure and conflict of interest

517 This work was supported by grants from the Swiss Neuromatrix
 518 Foundation, Switzerland and the Heffter Research Institute, USA; and
 519 by the Swiss National Science Foundation (A.S., No. 155184); K.F. was
 520 funded by a Wellcome Trust Principal research fellowship (Ref: 088130/Z/09/Z). The authors report no biomedical financial interests
 521 or potential conflicts of interest.
 522

523 Acknowledgments

524 We thank the staff at the Department of Psychiatry Psychotherapy
 525 and Psychosomatics for the medical and administrative support.

526 References

- 527 Ashburner, J., Friston, K.J., 2005. Unified segmentation. *Neuroimage* 26 (3), 839–851.
 528 <http://dx.doi.org/10.1016/j.neuroimage.2005.02.01815955494>.
- 529 Aznar, S., Klein, A.B., 2013. Regulating prefrontal cortex activation: an emerging role for
 530 the 5-HT_{2A} serotonin receptor in the modulation of emotion-based actions? *Mol.*
 531 *Neurobiol.* 48 (3), 841–853. <http://dx.doi.org/10.1007/s12035-013-8472-023696058>.
- 532 Dima, D., Stephan, K.E., Roiser, J.P., Friston, K.J., Frangou, S., 2011. Effective connectivity
 533 during processing of facial affect: evidence for multiple parallel pathways.
 534 *J. Neurosci.* 31 (40), 14378–14385. <http://dx.doi.org/10.1523/JNEUROSCI.2400-11.201121976523>.
- 535 Disner, S.G., Beevers, C.G., Haigh, E.A.P., Beck, A.T., 2011. Neural mechanisms of the cognitive
 536 model of depression. *Nat. Rev. Neurosci.* 12 (8), 467–477. <http://dx.doi.org/10.1038/nrn302721731066>.
- 537 First, M.B., Gibbon, M., Spitzer, R.L., Williams, J.B.W., Benjamin, L.S., 1997. Structured Clinical
 538 Interview for DSM-IV Axis II Personality Disorders (SCID-II). American Psychiatric
 539 Press, Inc., Washington, D.C.
- 540 Fisher, P.M., Meltzer, C.C., Price, J.C., Coleman, R.L., Ziolkowski, S.K., Becker, C., Moses-Kolko,
 541 E.L., Berga, S.L., Hariri, A.R., 2009. Medial prefrontal cortex 5-HT_{2A} density is correlated
 542 with amygdala reactivity, response habituation, and functional coupling. *Cereb.*
 543 *Cortex* 19 (11), 2499–2507. <http://dx.doi.org/10.1093/cercor/bhp02219321655>.
- 544 Freese, J.L., Amaral, D.G., 2005. The organization of projections from the amygdala to
 545 visual cortical areas TE and V1 in the macaque monkey. *J. Comp. Neurol.* 486 (4),
 546 295–317. <http://dx.doi.org/10.1002/cne.2052015846786>.
- 547 Frick, A., Howner, K., Fischer, H., Kristiansson, M., Furmark, T., 2013. Altered fusiform
 548 connectivity during processing of fearful faces in social anxiety disorder. *Transl.*
 549 *Psychiatry* 3, e312. <http://dx.doi.org/10.1038/tp.2013.8524105443>.
- 550 Friston, K.J., Harrison, L., Penny, W., 2003. Dynamic causal modelling. *Neuroimage* 19 (4),
 551 1273–1302. [http://dx.doi.org/10.1016/S1053-8119\(03\)00202-712948688](http://dx.doi.org/10.1016/S1053-8119(03)00202-712948688).
- 552 Friston, K.J., Holmes, A.P., Worsley, K.J., Poline, J.-P., Frith, C.D., Frackowiak, R.S.J., 1994. Statistical
 553 parametric maps in functional imaging: a general linear approach. *Hum. Brain*
 554 *Mapp.* 2 (4), 189–210. <http://dx.doi.org/10.1002/hbm.460020402>.
- 555 Furl, N., Henson, R.N., Friston, K.J., Calder, A.J., 2013. Top-down control of visual responses
 556 to fear by the amygdala. *J. Neurosci.* 33 (44), 17435–17443. <http://dx.doi.org/10.1523/JNEUROSCI.2992-13.201324174677>.
- 557 Goulden, N., McKie, S., Thomas, E.J., Downey, D., Juhasz, G., Williams, S.R., Rowe, J.B.,
 558 Deakin, J.F.W., Anderson, I.M., Elliott, R., 2012. Reversed frontotemporal connectivity

- during emotional face processing in remitted depression. *Biol. Psychiatry* 72 (7),
 559 604–611. <http://dx.doi.org/10.1016/j.biopsych.2012.04.03122682158>.
- 560 Grefkes, C., Wang, L.E., Eickhoff, S.B., Fink, G.R., 2010. Noradrenergic modulation of cortical
 561 networks engaged in visuospatial processing. *Cereb. Cortex* 20 (4), 783–797. <http://dx.doi.org/10.1093/cercor/bhp14419687293>.
- 562 Hahn, A., Stein, P., Windischberger, C., Weissenbacher, A., Spindelegger, C., Moser, E., Kasper,
 563 S., Lanzenberger, R., 2011. Reduced resting-state functional connectivity between amygdala
 564 and orbitofrontal cortex in social anxiety disorder. *Neuroimage* 56 (3), 881–889.
 565 Hariri, A.R., Mattay, V.S., Tessitore, A., Kolachana, B., Fera, F., Goldman, D., Egan, M.F.,
 566 Weinberger, D.R., 2002. Serotonin transporter genetic variation and the response of
 567 the human amygdala. *Science* 297 (5580), 400–403. <http://dx.doi.org/10.1126/science.107182912130784>.
- 568 Hasler, F., Grimberg, U., Benz, M.A., Huber, T., Vollenweider, F.X., 2004. Acute psychologi-
 569 cal and physiological effects of psilocybin in healthy humans: a double-blind,
 570 placebo-controlled dose-effect study. *Psychopharmacology (Berl.)* 172 (2),
 571 145–156. <http://dx.doi.org/10.1007/s00123-003-1640-614615876>.
- 572 Herrington, J.D., Taylor, J.M., Grupe, D.W., Curby, K.M., Schultz, R.T., 2011. Bidirectional
 573 communication between amygdala and fusiform gyrus during facial recognition.
 574 *Neuroimage* 56 (4), 2348–2355. <http://dx.doi.org/10.1016/j.neuroimage.2011.03.07221497657>.
- 575 Kastner, S., De Weerd, P., Desimone, R., Ungerleider, L.G., 1998. Mechanisms of directed
 576 attention in the human extrastriate cortex as revealed by functional MRI. *Science*
 577 282 (5386), 108–111. <http://dx.doi.org/10.1126/science.282.5386.1089756472>.
- 578 Komter, M., Schmidt, A., Bachmann, R., Studerus, E., Seifritz, E., Vollenweider, F.X., 2012.
 579 Psilocybin biases facial recognition, goal-directed behavior, and mood state toward
 580 positive relative to negative emotions through different serotonergic subreceptors.
 581 *Biol. Psychiatry* 72 (11), 898–906. <http://dx.doi.org/10.1016/j.biopsych.2012.04.00522578254>.
- 582 Kraehenmann, R., Preller, K.H., Scheidegger, M., Pokorny, T., Bosch, O.G., Seifritz, E.,
 583 Vollenweider, F.X., 2014. Psilocybin-induced decrease in amygdala reactivity correlates
 584 with enhanced positive mood in healthy volunteers. *Biol. Psychiatry*.
 585 Lang, P.J., Bradley, M.M., Cuthbert, B.N., 2005. International affective picture system
 586 (IAPS). Affective Ratings of Pictures and Instruction Manual. NIMH, Center for the
 587 Study of Emotion & Attention, Gainesville, FL CD-ROM.
- 588 Leuner, H., 1981. Halluzinogene. Psychische Grenzzustände in Forschung und
 589 Psychotherapie. Hans Huber, Bern, Stuttgart, Wien.
- 590 Lu, Q., Li, H., Luo, G., Wang, Y., Tang, H., Han, L., Yao, Z., 2012. Impaired prefrontal-
 591 amygdala effective connectivity is responsible for the dysfunction of emotion process
 592 in major depressive disorder: a dynamic causal modeling study on MEG. *Neurosci.*
 593 *lett.* 523 (2), 125–130. <http://dx.doi.org/10.1016/j.neulet.2012.06.05822750155>.
- 594 Morris, J.S., Friston, K.J., Büchel, C., Frith, C.D., Young, A.W., Calder, A.J., Dolan, R.J., 1998. A
 595 neuromodulatory role for the human amygdala in processing emotional facial ex-
 596 pressions. *Brain* 121 (1), 47–57. <http://dx.doi.org/10.1093/brain/121.1.479549487>.
- 597 Outhred, T., Hawkshead, B.E., Wager, T.D., Das, P., Malhi, G.S., Kemp, A.H., 2013. Acute
 598 neural effects of selective serotonin reuptake inhibitors versus noradrenaline
 599 reuptake inhibitors on emotion processing: implications for differential treatment ef-
 600 ficacy. *Neurosci. Biobehav. Rev.* 37 (8), 1786–1800. <http://dx.doi.org/10.1016/j.neubiorev.2013.07.01023886514>.
- 601 Penny, W.D., Stephan, K.E., Mechelli, A., Friston, K.J., 2004. Comparing dynamic causal
 602 models. *Neuroimage* 22 (3), 1157–1172. <http://dx.doi.org/10.1016/j.neuroimage.2004.03.02615219588>.
- 603 Pessoa, L., Adolphs, R., 2010. Emotion processing and the amygdala: from a 'low road' to
 604 'many roads' of evaluating biological significance. *Nat. Rev. Neurosci.* 11 (11),
 605 773–783. <http://dx.doi.org/10.1038/nrn292020959860>.
- 606 Rainnie, D.G., 1999. Serotonergic modulation of neurotransmission in the rat basolateral
 607 amygdala. *J. Neurophysiol.* 82 (1), 69–85. <http://dx.doi.org/10.1000936>.
- 608 Robinson, O.J., Overstreet, C., Allen, P.S., Letkiewicz, A., Vytal, K., Pine, D.S., Grillon, C., 2013. The
 609 role of serotonin in the neurocircuitry of negative affective bias: serotonergic modulation
 610 of the dorsal medial prefrontal-amygdala 'aversive amplification' circuit. *Neuroimage*
 611 78, 217–223. <http://dx.doi.org/10.1016/j.neuroimage.2013.03.07523583742>.
- 612 Schmidt, A., Komter, M., Bachmann, R., Seifritz, E., Vollenweider, F., 2013a. The NMDA
 613 antagonist ketamine and the 5-HT agonist psilocybin produce dissociative effects on
 614 structural encoding of emotional face expressions. *Psychopharmacology (Berl.)* 225
 615 (1), 223–239. <http://dx.doi.org/10.1007/s00213-012-2811-022836372>.
- 616 Schmidt, A., Smieskova, R., Aston, J., Simon, A., Allen, P., Fusar-Poli, P., McGuire, P.K.,
 617 Riecher-Rössler, A., Stephan, K.E., Borgwardt, S., 2013b. Brain connectivity abnormal-
 618 ities predating the onset of psychosis: correlation with the effect of medication.
 619 *J.A.M.A. Psychiatry* 70 (9), 903–912. <http://dx.doi.org/10.1001/jamapsychiatry.2013.11723824230>.
- 620 Sheehan, D.V., Lecrubier, Y., Sheehan, K.H., Amorim, P., Janavs, J., Weiller, E., Hergueta, T.,
 621 baker, Dunbar, R., 1998. The Mini-International Neuropsychiatric Interview (M.I.N.I.):
 622 the development and validation of a structured diagnostic psychiatric interview for
 623 DSM-IV and ICD-10. *Clin. Psychiatry* 59 (Suppl. 20), 22–33.
- 624 Sladky, R., Spies, M., Hoffmann, A., Kranz, G., Hummer, A., Gryglewski, G., Lanzenberger, R.,
 625 Windischberger, C., Kasper, S., 2015. (S)-citalopram Influences Amygdala Modulation
 626 in Healthy Subjects: A Randomized Placebo-controlled Double-blind fMRI Study
 627 Using Dynamic Causal Modeling 108, pp. 243–250.
- 628 Spielberger, C.D., Gorsuch, R.L., 1983. Manual for the State-Trait Anxiety Inventory (Form
 629 Y) ("Self-Evaluation Questionnaire") iv. Consulting Psychologists Press, Palo Alto, CA,
 630 p. 36.
- 631 Stephan, K.E., Penny, W.D., Daunizeau, J., Moran, R.J., Friston, K.J., 2009. Bayesian model
 632 selection for group studies. *Neuroimage* 46 (4), 1004–1017. <http://dx.doi.org/10.1016/j.neuroimage.2009.03.02519306932>.
- 633 Stephan, K.E., Weiskopf, N., Drysdale, P.M., Robinson, P.A., Friston, K.J., 2007. Comparing
 634 hemodynamic models with DCM. *Neuroimage* 38 (3), 387–401. <http://dx.doi.org/10.1016/j.neuroimage.2007.07.04017884583>.

- 648 Studerus, E., Komater, M., Hasler, F., Vollenweider, F.X., 2011. Acute, subacute and
649 long-term subjective effects of psilocybin in healthy humans: a pooled analysis of
650 experimental studies. *J. Psychopharmacol. (Oxford)* 25 (11), 1434–1452. <http://dx.doi.org/10.1177/026988111038246620855349>.
651
652 Vollenweider, F.X., Komater, M., 2010. The neurobiology of psychedelic drugs: implica-
653 tions for the treatment of mood disorders. *Nat. Rev. Neurosci.* 11 (9), 642–651.
654 <http://dx.doi.org/10.1038/nrn288420717121>.
655
656 Volman, I., Verhagen, L., den Ouden, H.E.M., Fernández, G., Rijpkema, M., Franke, B., Toni,
I., Roelofs, K., 2013. Reduced serotonin transporter availability decreases prefrontal
control of the amygdala. *J. Neurosci.* 33 (21), 8974–8979. <http://dx.doi.org/10.1523/JNEUROSCI.5518-12.201323699508>.
Vuilleumier, P., 2015. Affective and motivational control of vision. *Curr. Opin. Neurol.* 28
(1), 29–35. <http://dx.doi.org/10.1097/WCO.00000000000015925490197>.
Watson, D., Clark, L.A., Tellegen, A., 1988. Development and validation of brief measures of
positive and negative affect: the PANAS scales. *J. Pers. Soc. Psychol.* 54 (6),
1063–1070. <http://dx.doi.org/10.1037/0022-3514.54.6.10633397865>.

UNCORRECTED PROOF